NASA TECHNICAL MEMORANDUM

NASA TM 73,244

(NASA-TM-X-73244) HELICOPTER OPTIMAL DESCENT AND LANDING AFTER POWER LOSS (NASA) 33 p HC A03/MF A01 CSCL 01A

N77-26067

Unclas
G3/01 35456

NASA TM 73,244

HELICOPTER OPTIMAL DESCENT AND LANDING AFTER POWER LOSS

Wayne Johnson

Ames Research Center

and

Ames Directorate, USAAMRDL
Ames Research Center
Moffett Field, Calif. 94035

May 1977

1. Report No. NASA TM 73,244	2. Government Accession No.	3. Recipient's Catalog No.

4. Title and Subtitle HELICOPTER OPTIMAL DESCENT AND LANDING AFTER POWER LOSS	5. Report Date 6. Performing Organization Code
7. Author(s) Wayne Johnson	8. Performing Organization Report No. A-7047
9. Performing Organization Name and Address Ames Research Center, and Ames Directorate, USAAMRDL Ames Research Center, Moffett Field, Calif. 94035	10. Work Unit No. 505-10-22 11. Contract or Grant No.
12. Sponsoring Agency Name and Address National Aeronautics and Space Administration, Washington, D.C. 20546 and U.S. Army Air Mobility R&D Laboratory, Moffett Field, Calif. 94035	13. Type of Report and Period Covered Technical Memorandum 14. Sponsoring Agency Code

15. Supplementary Notes

16. Abstract

An optimal control solution is obtained for the descent and landing of a helicopter after the loss of power in level flight. The model considers the helicopter vertical velocity, horizontal velocity, and rotor speed; and it includes representations of ground effect, rotor inflow time lag, pilot reaction time, rotor stall, and the induced velocity curve in the vortex ring state. The control (rotor thrust magnitude and direction) required to minimize the vertical and horizontal velocity at contact with the ground is obtained using nonlinear optimal control theory. It is found that the optimal descent after power loss in hover is a purely vertical flight path. Good correlation, even quantitatively, is found between the calculations and (non-optimal) flight test results. The optimal control solution is thus a consistent and accurate method for comparing and evaluating the power-off descent characteristics of various helicopter designs.

17. Key Words (Suggested by Author(s)) Helicopter autorotation Nonlinear optimal control	18. Distribution Statement Unlimited STAR Category - 01

19. Security Classif. (of this report)	20. Security Classif. (of this page)	21. No. of Pages	22. Price*
Unclassified	Unclassified	33	$3.75

*For sale by the National Technical Information Service, Springfield, Virginia 22161

NOMENCLATURE

a	rotor blade two-dimensional lift curve slope
A	rotor disk area, πR^2
c	rotor blade chord
c_d	rotor blade section drag coefficient (at zero lift)
C_Q	rotor torque coefficient, $Q/\rho AR(\Omega R)^2$
C_T	rotor thrust coefficient, $T/\rho A(\Omega R)^2$
C_{T_o}	initial thrust coefficient, $W/\rho A(\Omega_o R)^2$
C_T/σ_s	rotor stall limit
C_x	$C_T \sin\alpha$
C_z	$C_T \cos\alpha$
d	$\dot{h}/\Omega_o R$
D	helicopter parasite drag
e	$\dot{x}/\Omega_o R$
f	helicopter equivalent parasite drag area
f_G	ground effect factor in induced velocity
$f_I(x,y)$	induced velocity curve
g	acceleration due to gravity
g_o	$g/\Omega_o^2 R$
h	helicopter vertical position coordinate (measured downward from the initial altitude)
h_o	helicopter altitude above ground at power loss
$\dot{h}_f$	vertical velocity at ground contact
I_b	rotor blade flap inertia
I_R	total rotor rotational inertia, NI_b
J	optimal control cost function
l	$v/\Omega_o R$
M	helicopter mass
N	number of blades
n_s	stall parameter
n_z	helicopter vertical load factor
Q	rotor torque
R	rotor blade radius
t	time
T	rotor thrust

v	rotor induced velocity
v_h	$(T/2\rho A)^{\frac{1}{2}}$
V	$(\dot{x}^2 + \dot{h}^2)^{\frac{1}{2}}$
V_f	helicopter velocity at ground contact
W	helicopter gross weight
W_x	weighting factor in J, on horizontal velocity relative to vertical velocity
x	helicopter horizontal position coordinate
x	vertical velocity parameter in inflow curve
$\dot{x}_f$	horizontal velocity at ground contact
y	horizontal velocity parameter in inflow curve
α	angle of rotor thrust vector from vertical
γ	rotor Lock number, $\rho acR^4/I_b$
θ	angle of helicopter velocity from horizontal, $\tan^{-1}(-\dot{h}/\dot{x})$
θ_{75}	rotor collective pitch
κ	empirical factor on induced velocity
λ	rotor inflow ratio (tip-path-plane reference)
λ_h	$(C_T/2)^{\frac{1}{2}}$
μ	rotor advance ratio (tip-path-plane reference)
ρ	air density
σ	rotor solidity ratio, $Nc/\pi R$
τ	induced velocity time lag
τ_o	$\Omega_o \tau$
ω	Ω/Ω_o
Ω	rotor rotational speed
Ω_o	initial value of rotor rotational speed
$(\ )_o$	initial value
$(\ )^{\bullet}$	$d(\ )/dt$
$(\ )^{\triangledown}$	$d(\ )/dh$

HELICOPTER OPTIMAL DESCENT AND LANDING AFTER POWER LOSS

Wayne Johnson*

Ames Research Center
and
Ames Directorate, USAAMRDL

SUMMARY

An optimal control solution is obtained for the descent and landing of a helicopter after the loss of power in level flight. The model considers the helicopter vertical velocity, horizontal velocity, and rotor speed; and it includes representations of ground effect, rotor inflow time lag, pilot reaction time, rotor stall, and the induced velocity curve in the vortex ring state. The control (rotor thrust magnitude and direction) required to minimize the vertical and horizontal velocity at contact with the ground is obtained using nonlinear optimal control theory. It is found that the optimal descent after power loss in hover is a purely vertical flight path. Good correlation, even quantitatively, is found between the calculations and (non-optimal) flight test results. The optimal control solution is thus a consistent and accurate method for comparing and evaluating the power-off descent characteristics of various helicopter designs.

INTRODUCTION

Good autorotation characteristics during descent after power loss are essential for a useful and safe helicopter design. While it is known that the helicopter rotor has a minimum descent rate in vertical autorotation about the same as a parachute of equal size, there are other questions which require consideration. First, the helicopter rotor is a rather small parachute, so the ideal descent rate can be fairly high ($V \cong 1.16(T/A)^{\frac{1}{2}}$ m/sec, where T/A is the disk loading in kg/m^2). This high basic descent rate increases

*Research Scientist, Large Scale Aerodynamics Branch, NASA-Ames Research Center the importance of other parameters in the power-off landing maneuver. Secondly, it is necessary to fly the helicopter in a manner to achieve the least descent rate, and most importantly to flare near the ground so that the helicopter touches down with vertical and horizontal velocities as nearly zero as possible.

It is desirable to have in the preliminary design process a means of assessing the influence of basic parameters on the helicopter autorotation characteristics. A number of elementary autorotation indices have been developed, generally based on the ratio of the rotor kinetic energy to the helicopter power required, KE/P (KE is the energy available during the descent, and P is the rate of energy decrease just after the loss of engine power, thus a high ratio of KE/P is desired). The problem is more complex really, with many parameters of the helicopter design influencing the autorotation characteristics. A difficulty lies in the necessity for flying the helicopter to the ground, which requires the choice of a control schedure. A poor choice for the helicopter control can easily result in an unacceptable landing, thus obscuring the influence of the design parameters. Therefore this report considers the use of nonlinear optimal control theory to establish the best control schedule, and thereby eliminate the influence of the control choice. The result is a consistent method for comparing and evaluating the power-off landing characteristics of various helicopter designs.

EQUATIONS OF MOTION

The optimization problem to be formulated is to find the control after power loss to arrive at the ground with minimum velocity, given the helicopter initial altitude h_0, flight state, and basic parameters. The helicopter is assumed to be in equilibrium level flight at the instant of power loss, with rotational speed Ω_0, rotor loading $(C_T/\sigma)_0$, and forward speed μ_0. The basic parameters of the helicopter design include the Lock number γ, the rotor radius R, and the solidity ratio σ. The aircraft position is defined by the coordinates h and x, respectively vertical and horizontal (see figure 1). It is convenient to measure h downward, so $h = 0$ at the initial altitude and $h = h_0$ at the ground.

The optimal control problem is best solved using an independent variable which has a fixed end point. Thus the independent variable for the present problem must be the height h rather than time, since the arrival at the ground is defined by $h = h_0$ at an unknown time. The change of variables is accomplished using $d(\ \ )/dt = \dot{h}\, d(\ \ )/dh$, or $(\ \ )^{\cdot} = \dot{h}\,(\ \ )^{\triangledown}$. The numerical integration which is required to solve the problem is still best done with respect to time however (see below).

For the control variables, the magnitude and direction of the rotor thrust are used, specifically the thrust coefficient C_T and the angle of the thrust vector to the vertical α (see figure 1). It is convenient to express the problem in terms of the vertical and horizontal components of C_T, $C_z = C_T \cos\alpha$ and $C_x = C_T \sin\alpha$ respectively. The collective pitch control required to obtain this thrust may be then obtained from the blade element theory expression

$$\theta_{75} = \frac{(1+\frac{3}{2}\mu^2)\frac{6C_T}{\sigma a} + \frac{3}{2}\lambda(1-\frac{1}{2}\mu^2)}{1-\mu^2+\frac{9}{4}\mu^4}$$

It is not possible to obtain the longitudinal cyclic control from α without considering the helicopter pitch attitude and the rotor flapping also; the primary interest here is in the flight path anyway.

The equations of motion considered to describe the helicopter descent after power loss are those for vertical descent velocity $\dot{h}$, horizontal velocity $\dot{x}$, rotor speed Ω, and induced velocity v. A separate differential equation is used for the induced velocity partly to allow consideration of a time lag in the inflow response, and partly to simplify the incorporation of the inflow curve (including ground effect) in the model. Vertical force equilibrium (see figure 1) gives:

$$M\ddot{h} = W - T\cos\alpha + D\sin\theta$$

or since $W = Mg$ and $\ddot{h} = \dot{h}\frac{\partial}{\partial h}\dot{h}$,

$$\dot{h}' = \frac{g}{\dot{h}}\left(1 - \frac{T\cos\alpha}{W} + \frac{D\sin\theta}{W}\right)$$

Horizontal force equilibrium gives

$$M\ddot{x} = T\sin\alpha - D\cos\theta$$

or

$$\dot{x}' = \frac{g}{\dot{h}}\left(\frac{T\sin\alpha}{W} - \frac{D\cos\theta}{W}\right)$$

The helicopter parasite drag will be defined by an equivalent area f, such that $D = \frac{1}{2}\rho V^2 f$; then $D\sin\theta = -\frac{1}{2}\rho\dot{h}(\dot{h}^2+\dot{x}^2)^{\frac{1}{2}}f$, and $D\cos\theta = \frac{1}{2}\rho\dot{x}(\dot{h}^2+\dot{x}^2)^{\frac{1}{2}}f$ (see figure 1). Rotor torque equilibrium after the loss of engine power is:

$$I_R\dot{\Omega} = -Q$$

or

$$\Omega' = -\frac{Q}{I_R\dot{h}}$$

where Q is the rotor aerodynamic torque, given by

$$\frac{C_Q}{\sigma} = \frac{c_d}{8}\left(1 + \left(6\frac{C_T}{\sigma}\right)^2 + \left(\frac{C_T/\sigma}{C_T/\sigma_s}\right)^{n_s}\right)(1+4.6\mu^2) + \frac{C_T}{\sigma}\lambda$$

(reference 1). Here C_T/σ_s is the rotor stall limit (with n_s a large number, e.g. $n_s = 20$, so the profile torque greatly increases when the loading is above C_T/σ_s). The rotor advance ratio μ and inflow ratio λ are given by

$$\mu = \frac{\dot{x}\cos\alpha + \dot{h}\sin\alpha}{\Omega R}$$

$$\lambda = \frac{\dot{x}\sin\alpha - \dot{h}\cos\alpha + v}{\Omega R}$$

The rotor induced velocity v is given by a differential equation which includes a time lag τ :

$$\tau\dot{v} + v = \kappa v_h f_I f_G$$

or

$$V^{v} = \frac{-v + \kappa v_h f_I f_G}{\tau \dot{h}}$$

The steady state solution is thus $v = \kappa v_h f_I f_G$.
Here $v_h^2 = T/2\rho A$, κ is an empirical factor (typically $\kappa = 1.15$), f_I is the inflow curve, and f_G is the effect of the ground.

For the inflow curve, the following expression is used:

$$f_I(x,y) = \begin{cases} \dfrac{1}{\sqrt{y^2 + (x + f_I)^2}} & \text{if } (2x+3)^2 + y^2 > 1 \\ x(.373x^2 + .598y^2 - 1.991) & \text{if } (2x+3)^2 + y^2 \leq 1 \end{cases}$$

where the parameters x and y are defined by

$$x = \frac{\lambda_c}{\lambda_h} = \frac{\dot{x}\sin\alpha - \dot{h}\cos\alpha}{v_h}$$

$$y = \frac{\mu}{\lambda_h} = \frac{\dot{x}\cos\alpha + \dot{h}\sin\alpha}{v_h}$$

The first expression for f_I is the usual momentum theory result (ref. 1); the second expression is an empirical approximation for the vortex ring state (where the momentum theory breaks down). The region of roughness in the vortex ring state is defined approximately by $(2x+2)^2+y^2<1$. To account for ground effect, the following expression is used (ref. 2):

$$f_G = 1 - \frac{\cos^2\epsilon}{(4z)^2}$$

Here z is the rotor height above the ground, $z = h_o - h + z_o$ (z_o is the rotor height for the aircraft on the ground); and ϵ is the angle of the wake to the ground,

$$\cos^2\epsilon = \frac{(-\dot{h} + v\cos\alpha)^2}{(-\dot{h} + v\cos\alpha)^2 + (\dot{x} + v\sin\alpha)^2}$$

DIMENSIONLESS EQUATIONS

Now the equations will be made dimensionless using the quantities g, Ω_o, and R. The four degrees of freedom are defined as follows:

$$d = \dot{h}/\Omega_o R$$
$$e = \dot{x}/\Omega_o R$$
$$\omega = \Omega/\Omega_o$$
$$\ell = v/\Omega_o R$$

and the control variables are $C_z = C_T \cos\alpha$ and $C_x = C_T \sin\alpha$. The four differential equations are then:

$$d' = \frac{g_o}{d}\left(1 - \frac{C_z}{C_{T_o}}\omega^2 - \frac{\frac{1}{2}f/A}{C_{T_o}} d\sqrt{d^2+e^2}\right)$$

$$e' = \frac{g_o}{d}\left(\frac{C_x}{C_{T_o}}\omega^2 - \frac{\frac{1}{2}f/A}{C_{T_o}} e\sqrt{d^2+e^2}\right)$$

$$\omega' = -\frac{\gamma}{a}\frac{\omega^2}{d}\left[\frac{C_d}{8}\left(1+\left(16\frac{C_T}{\sigma}\right)^2+\left(\frac{C_T/\sigma}{C_T/\sigma_s}\right)^{ns}\right)\left(1+4.6\mu^2\right)+\frac{C_T}{\sigma}\lambda\right]$$

$$\ell' = \frac{1}{\tau_0 d}\left[-\ell + K\lambda_h \omega f_I f_G\right]$$

where $g_0 = g/\Omega_0^2 R$, $\tau_0 = \Omega_0 \tau$, $\lambda_h = (C_T/2)^{\frac{1}{2}}$, $C_{T_0} = W/\rho A(\Omega_0 R)^2$; and

$$\mu = \frac{1}{\omega C_T}\left[eC_z + dC_x\right]$$

$$\lambda = \frac{1}{\omega C_T}\left[eC_x - dC_z\right] + \frac{\ell}{\omega}$$

For f_I and f_G in the inflow equation, the following quantities are required:

$$x = \frac{eC_x - dC_z}{\omega C_T^{3/2}/\sqrt{2}}$$

$$y = \frac{eC_z + dC_x}{\omega C_T^{3/2}/\sqrt{2}}$$

$$\cos^2\epsilon = \frac{(-dC_T + \ell C_z)^2}{(-dC_T + \ell C_z)^2 + (eC_T + \ell C_x)^2}$$

Finally, the initial conditions (for level flight) are $d = 0$, $e = \mu_0$, $\omega = 1$, and $\ell = \ell_0 = v_0/\Omega_0 R$ at $h = 0$.

CRITERION

The optimization problem is to arrive at the ground with minimum vertical and horizontal velocity. Thus a quadratic cost function of the following form is used:

$$J = \tfrac{1}{2}\left(\dot{h}_f^2 + W_x \dot{x}_f^2\right)$$

where $\dot{h}_f$ and $\dot{x}_f$ are the velocities at the ground ($h = h_o$), and W_x is the weighting function of horizontal velocity relative to vertical velocity. Now since $\ddot{h} = \frac{d}{dh}(\frac{1}{2}\dot{h}^2) = g(1 - T\cos\alpha/W + D\sin\theta/W)$, there follows

$$\frac{1}{2}\dot{h}^2 = g\int_0^h \left(1 - \frac{T\cos\alpha}{W} + \frac{D\sin\theta}{W}\right) dh$$

and similarly

$$\frac{1}{2}\dot{x}^2 = \frac{1}{2}\dot{x}_o^2 + \int_0^x \ddot{x}\, dx = \frac{1}{2}\dot{x}_o^2 + \int_0^h \frac{\dot{x}}{\dot{h}}\ddot{x}\, dh$$

$$= \frac{1}{2}\dot{x}_o^2 + g\int_0^h \frac{\dot{x}}{\dot{h}}\left(\frac{T\sin\alpha}{W} - \frac{D\cos\theta}{W}\right) dh$$

So an equivalent cost function is:

$$J = g\int_0^{h_o}\left[\left(1 - \frac{T\cos\alpha}{W} + \frac{D\sin\theta}{W}\right) + W_x\frac{\dot{x}}{\dot{h}}\left(\frac{T\sin\alpha}{W} - \frac{D\cos\theta}{W}\right)\right] dh$$

in terms of the dimensionless quantities then,

$$J = g_o\int_0^{h_o}\left[\left(1 - \frac{C_z}{C_{T_o}}\omega^2 - \frac{\frac{1}{2}f/A}{C_{T_o}} d\sqrt{d^2+e^2}\right)\right.$$
$$\left. + W_x\frac{e}{d}\left(\frac{C_x}{C_{T_o}}\omega^2 - \frac{\frac{1}{2}f/A}{C_{T_o}} e\sqrt{d^2+e^2}\right)\right] dh$$

The control problem is to find C_z and C_x as a function of h to minimize J, subject to the constraints defined by the differential equations above.

NONLINEAR OPTIMAL CONTROL

Consider a system defined by the nonlinear differential equation $\vec{x}' = \vec{a}(\vec{x}, \vec{u}, h)$, where $\vec{x}$ is the state vector, $\vec{u}$ is the control vector, and h is the independent variable; and a cost function $J = \int_{h_i}^{h_f} b(\vec{x}, \vec{u}, h)\, dh$. It is assumed that the initial conditions $\vec{x}(h_i)$ are given, and that h_i and h_f are fixed. The optimal control problem is to find $\vec{u}(h)$ to minimize J. The solution (see reference 3) is defined by the following set of equations:

$$\vec{x}' = \vec{a}$$

$$\vec{p}' = -\left(\frac{\partial \vec{a}}{\partial \vec{x}}\right)^T \vec{p} - \frac{\partial b}{\partial \vec{x}}$$

$$\frac{\partial H}{\partial \vec{u}} = \left(\frac{\partial \vec{a}}{\partial \vec{u}}\right)^T \vec{p} + \frac{\partial b}{\partial \vec{u}} = 0$$

with boundary conditions $x(h_i) = x_i$ and $p(h_f) = 0$.

For simple problems, the equation $\partial H/\partial \vec{u} = 0$ is solved directly for $\vec{u}$ as a function of $\vec{x}$, $\vec{p}$, and h; and $\vec{u}$ is substituted into the first two equations. The differential equations are then integrated, using the boundary conditions to eliminate integration constants. Then the solution for $\vec{x}$ is the optimal path, and $\vec{p}$ gives the optimal control law $\vec{u}(h)$.

The present problem is too complex for such a procedure, so a steepest descent algorithm is used to solve the two point boundary value problem (reference 3). A cycle in the algorithm consists of the following steps. A current estimate of the optimal control law, $\vec{u}^{(n)}$, is available. The differential equation $\vec{x}' = \vec{a}$ is integrated forward from h_i to h_f using $\vec{u}^{(n)}$ and the initial consitions on $\vec{x}$. Next the differential equation $\vec{p}' = -\partial H/\partial \vec{x}$ is integrated backward from h_f to h_i using $\vec{x}$, $\vec{u}^{(n)}$, and the final conditions on $\vec{p}$. Finally, $(\partial H/\partial \vec{u})^{(n)}$ is evaluated using $\vec{x}$, $\vec{p}$, and $\vec{u}^{(n)}$; and the control is incremented by

$$\vec{u}^{(n+1)} = \vec{u}^{(n)} - \lambda \frac{\partial H}{\partial \vec{u}}^{(n)}$$

where λ is a step size, chosen (by trial and error) such that the solution converges fast enough without overshooting. This process is repeated until the solution converges to the optimum, as indicated by the cost J approaching a minimum. Such a steepest descent procedure has the advantage of not being sensitive to the initial guess for the control; the convergence slows down as the minimum is approached however.

OPTIMAL CONTROL PROBLEM

The optimal control problem for the power-off descent and landing of a helicopter is obtained by applying nonlinear optimal control theory to the dimensionless equations given above. The formulation using h as the independent variable is required since the final height is specified, rather than the final time. It is still preferable to do the actual numerical integration using time as the independent variable however, to eliminate the singularity which occurs at d = 0 (such as at the start of the maneuver) is h is the independent variable. Therefore after the differential equation for $\vec{p}$ is opbtained, the coordinate transformation is made back to t, using $d(\ )^{\blacktriangledown} = (\ )^{\cdot}$. It is also necessary then to integrate $\dot{h} = d\Omega_0 R$ to obtain the proper variable h (and also $\dot{x} = e\Omega_0 R$ to obtain x(t)). The resulting system of equations for the optimal control problem is then as follows.

A)

$$d^{\circ} = g_0 \left(1 - \frac{C_z}{C_{T_0}} \omega^2 - \frac{\frac{1}{2} f/A}{C_{T_0}} d\sqrt{d^2+e^2} \right)$$

$$e^{\circ} = g_0 \left(\frac{C_x}{C_{T_0}} \omega^2 - \frac{\frac{1}{2} f/A}{C_{T_0}} e\sqrt{d^2+e^2} \right)$$

$$\omega^{\circ} = -\frac{\gamma}{\sigma} \omega^2 \left[\frac{c_d}{8} \left(1 + \left(6\frac{C_T}{\sigma}\right)^2 + \left(\frac{C_T/\sigma}{C_T/\sigma_s}\right)^{n_s}\right)(1+4.6\mu^2) + \frac{C_T}{\sigma}\lambda \right]$$

$$\lambda^{\circ} = \frac{1}{\tau} \left[-\ell + K\lambda_h \omega f_I f_G \right]$$

B)

$$\begin{pmatrix} p_d \\ p_e \\ p_\omega \\ p_\ell \end{pmatrix}^{\circ} = -B \begin{pmatrix} p_d \\ p_e \\ p_\omega \\ p_\ell \end{pmatrix} + \begin{bmatrix} g_0 \frac{\frac{1}{2} \xi \ell A}{C_{T_0}} d \left(\frac{2d^2 + e^2 - W_x e^4 / d^2}{\sqrt{d^2+e^2}} \right) + g_0 W_x \frac{e}{d} \frac{C_x}{C_{T_0}} \omega^2 \\ g_0 \frac{\frac{1}{2} k \ell A}{C_{T_0}} \left(\frac{d^2 e + W_x (2ed^2 + 3e^3)}{\sqrt{d^2+e^2}} \right) - g_0 W_x \frac{C_x}{C_{T_0}} \omega^2 \\ - g_0 2 \omega d \left(- \frac{C_z}{C_{T_0}} + W_x \frac{e}{d} \frac{C_x}{C_{T_0}} \right) \\ 0 \end{bmatrix}$$

C)

$$\begin{pmatrix} \frac{\partial H}{\partial C_z} \\ \frac{\partial H}{\partial C_x} \end{pmatrix} = C \begin{pmatrix} p_d \\ p_e \\ p_\omega \\ p_\ell \end{pmatrix} + \begin{bmatrix} - g_0 \frac{\omega^2}{C_{T_0}} d \\ W_x g_0 \frac{\omega^2}{C_{T_0}} e \end{bmatrix}$$

D) at $h = 0$: $d = 0$, $e = \mu_0$, $\omega = 1$, $\ell = \ell_0$

at $h = h_0$: $p_d = p_e = p_\omega = p_\ell = 0$

where

$$Q_0 = \frac{C_d}{8} \left[1 + \left(6 \frac{C_T}{\sigma}\right)^2 + \left(\frac{C_T/\sigma}{C_T/\sigma_s} \right)^{n_s} \right]$$

$$Q_1 = \frac{C_d}{8} \left[72 \frac{C_T}{\sigma} + \frac{n_s}{C_T/\sigma_s} \left(\frac{C_T/\sigma}{C_T/\sigma_s} \right)^{n_s - 1} \right] \frac{1 + 4.6 \mu^2}{\sigma}$$

$$\xi_d = K \lambda_h \omega \xi_I \xi_G + K d \xi_G \left(\frac{\partial \xi_I}{\partial x} \frac{C_z}{C_T} - \frac{\partial \xi_I}{\partial y} \frac{C_x}{C_T} \right)$$

$$\xi_e = K e \xi_G \left(\frac{\partial \xi_I}{\partial x} \frac{C_x}{C_T} + \frac{\partial \xi_I}{\partial y} \frac{C_z}{C_T} \right)$$

and the matrices B and C are defined as follows.

$$
B = \begin{bmatrix}
-\frac{g_0}{d}\left(1-\frac{C_z}{C_{T_0}}\omega^2\right) - g_0\frac{\frac{1}{2}\xi|A}{C_{T_0}}\frac{d^2}{\sqrt{d^2+e^2}} & -\frac{g_0}{d}\frac{C_x}{C_{T_0}}\omega^2 + g_0\frac{\frac{1}{2}\xi|A}{C_{T_0}}\frac{e^2}{d\sqrt{d^2+e^2}} & \frac{\gamma}{a}\frac{\omega^2}{d}Q_0(1+4.6\mu^2) - \frac{\gamma}{a}\omega Q_0\, 9.2\mu\frac{C_x}{C_T} + \frac{\gamma}{a}\frac{\omega}{d}\left(\ell\frac{C_T}{\sigma}+e\frac{C_x}{\sigma}\right) & \frac{\ell-f_d}{\tau_0 d} + \frac{k\lambda_h\omega f_I}{\tau_0}\frac{\partial f_G}{\partial d} \\
-g_0\frac{\frac{1}{2}\xi|A}{C_{T_0}}\frac{ed}{\sqrt{d^2+e^2}} & -g_0\frac{\frac{1}{2}\xi|A}{C_{T_0}}\frac{d^2+2e^2}{\sqrt{d^2+e^2}} & -\frac{\gamma}{a}\omega Q_0\, 9.2\mu\frac{C_z}{C_T} - \frac{\gamma}{a}\omega\frac{C_x}{\sigma} & \frac{f_e}{\tau_0 e} + \frac{k\lambda_h\omega f_I}{\tau_0}\frac{\partial f_G}{\partial e} \\
-g_0 2\omega\frac{C_z}{C_{T_0}} & g_0 2\omega\frac{C_x}{C_{T_0}} & -\frac{\gamma}{a}2\omega Q_0 - \frac{\gamma}{a}\left(\ell\frac{C_T}{\sigma} - d\frac{C_z}{\sigma} + e\frac{C_x}{\sigma}\right) & \frac{f_d-f_e}{\tau_0\omega} \\
0 & 0 & -\frac{\gamma}{a}\omega\frac{C_T}{\sigma} & -\frac{1}{\tau_0} + \frac{k\lambda_h\omega f_I}{\tau_0}\frac{\partial f_G}{\partial \ell}
\end{bmatrix}
$$

$$
C = \left[\begin{array}{c|c|c|c}
-g_0 \frac{\omega^2}{C_{T_0}} & 0 & \begin{array}{l} -\frac{\gamma}{a}\omega^2 Q_1 \frac{C_z}{C_T} \\ -\frac{\gamma}{a}\omega\, Q_0\, 9.2\mu\, \frac{eC_x^2 - dC_xC_z}{C_T^3} \\ -\frac{\gamma}{a}\frac{\omega}{\sigma}\left(l\frac{C_z}{C_T} - d\right) \end{array} & \begin{array}{l} \frac{k\omega\xi_I}{\tau_0}\left[\xi_G \frac{C_z}{4\lambda_h C_T} + \lambda_h \frac{\partial \xi_G}{\partial C_z}\right] \\ + \frac{k\xi_G}{\tau_0}\frac{\partial \xi_I}{\partial x}\left(-\frac{d}{C_T} - \frac{3}{2}\,\frac{eC_xC_z - dC_z^2}{C_T^3}\right) \\ + \frac{k\xi_G}{\tau_0}\frac{\partial \xi_I}{\partial y}\left(\frac{e}{C_T} - \frac{3}{2}\,\frac{eC_z^2 + dC_xC_z}{C_T^3}\right) \end{array} \\
\hline
0 & g_0 \frac{\omega^2}{C_{T_0}} & \begin{array}{l} -\frac{\gamma}{a}\omega^2 Q_1 \frac{C_x}{C_T} \\ -\frac{\gamma}{a}\omega\, Q_0\, 9.2\mu\, \frac{dC_z^2 - eC_xC_z}{C_T^3} \\ -\frac{\gamma}{a}\frac{\omega}{\sigma}\left(l\frac{C_x}{C_T} + e\right) \end{array} & \begin{array}{l} \frac{k\omega\xi_I}{\tau_0}\left[\xi_G \frac{C_x}{4\lambda_h C_T} + \lambda_l \frac{\partial \xi_G}{\partial C_x}\right] \\ + \frac{k\xi_G}{\tau_0}\frac{\partial \xi_I}{\partial x}\left(\frac{e}{C_T} - \frac{3}{2}\,\frac{eC_x^2 - dC_xC_z}{C_T^3}\right) \\ + \frac{k\xi_G}{\tau_0}\frac{\partial \xi_I}{\partial y}\left(\frac{d}{C_T} - \frac{3}{2}\,\frac{eC_xC_z + dC_x^2}{C_T^3}\right) \end{array}
\end{array}\right]
$$

These equations are solved by the steepest descent method outlined above. The pilot reaction time t_p is included by constraining the collective pitch to have the initial value for $t < t_p$. Then the control is given by

$$C_T = \frac{\sigma a}{6} \; \frac{(1-\mu^2+\frac{9}{4}\mu^4)(\theta_{75})_o - \frac{3}{2}\lambda(1-\frac{1}{2}\mu^2)}{1+\frac{3}{2}\mu^2}$$

Assuming α is unchanged for $t < t_p$, then $C_x/C_z = C_{x_o}/C_{z_o} = (\frac{1}{2}f/A\mu_o^2)/C_{T_o}$. Typically $t_p \cong .75$ sec (although handling qualities specifications may require the use of a larger value).

DESCENT FROM HOVER

Consider the case of optimal descent after power loss in hover, hence with initial condition $\mu_o = 0$. The solution of the above equations will be shown to be $C_x = 0$ and $e = 0$ ($\alpha = 0$ and $\dot{x} = 0$).

Assuming $C_x = e = 0$, it follows that $\mu = 0$, $y = 0$, $\partial f_I/\partial y = 0$ (i.e. $\partial\lambda_i/\partial\mu = 0$ at $\mu = 0$), and f_G is a function of h only. The differential equation for e becomes $\dot{e} = 0$, with solution e = constant = 0 (using the initial condition $e = \mu_o = 0$). The differential equation above for p_e becomes then $p_e^{\nabla} = g_o(\frac{1}{2}\frac{f}{A}/C_{T_o})p_e$, which has solution

$$p_e = p_e(h_o)\exp\left[g_o\frac{\frac{1}{2}f/A}{C_{T_o}}(h-h_o)\right]$$

or $p_e \equiv 0$ since the final conditions on $\vec{p}$ give $p_e(h_o) = 0$. Then $\partial H/\partial C_x = g_o(\omega^2/d\,C_{T_o})p_e \equiv 0$, as required for the optimal solution. The remaining problem has then only three degrees of freedom (d, ω, and Ω), one control variable ($C_z = C_T$), and threee components of $\vec{p}$ (p_d, p_ω, and p_Ω). While eliminating e, C_x, and p_e from the problem is a significant simplification, it is still necessary to integrate numerically and iterate to find the optimal solution.

Thus the optimal control solution for descent from howver after power loss is a purely vertical flight path. The same conclusion was reached from the flight tests reqorted in reference 4, although in practice a small amount of forward speed is required, both to avoid the vortex ring state during flare and to keep the landing point in sight.

RESULTS AND DISCUSSION

The optimal descent of a helicopter after power loss has been calculated for a number of cases. Because it is found both by flight tests and from calculations that an initial forward velocity greatly improves the autorotation characteristics, results are given here only for descent from power loss in hover (which as found above involves a purely vertical flight path). The helicopter considered is one for which flight test data are available. Three values of the rotor Lock number are considered, from $\gamma = 4.5$ (the standard rotor) to $\gamma = 2.6$ (a rotor with heavier blades, investigated specifically for better autorotation characteristics). Figure 2 shows the vertical velocity at the instant of contact with the ground, after optimal descent from power loss in hover at varous altitudes. These calculations are in agreement with the flight test results. Specifically, it was found in reference 4 that the autorotation characteristics greatly improved for the heavier rotor (the autorotation characteristics for the helicopter with $\gamma = 4.5$ are poor in this altitude range, while the characteristics of the helicopter with $\gamma = 2.6$ were found to be very good); and the critical height with $\gamma = 2.6$ was about $h_o = 30m$.

Figure 3 presents in detail the optimal solution for power-off descent from hover at an altitude of $h_o = 30m$. Figure 3(a) gives the collective pitch control required as a function of time (note that a pilot reaction time of .75 sec is used). These results again agree generally with reference 4, which found in flight tests that the collective should be dropped immediately, followed by a gradual increase for flare (in figure 3(a) the flare begins when the helicopter is about 20m above the ground). Figure 3(b) shows the rotor C_T/σ as a function of altitude (the control variable actually used in the solution procedure). A stall limit of $C_T/\sigma_s = .15$ was used, which results in a leveling off of the control just before it reaches that value; the high torque due to rotor stall greatly slows down the rotor, and thus values of C_T/σ above stall are not called for until just before ground contact. Figure 3(c) shows the helicopter vertical load factor ($n_z = [C_T\omega^2 + \frac{1}{2} f/A\, \lambda(\lambda^2+\mu^2)^{\frac{1}{2}}]/C_{T_0}$;

figure 3(d) shows the rotor speed, as a fraction of the initial value; and figure 3(e) shows the vertical descent velocity (the rotor is operating in the windmill brake state when the velocity is increasing, and in the vortex ring state at the end of the maneuver when the velocity is decreasing). Finally, figure 3(f) presents the flight path for the optimal descent; note that the principal influence of Lock number is on the final portion of the flare for these cases, where the extra kinetic energy in the heavier rotor allows a greater reduction in velocity.

Figures 4 and 5 present a comparison between flight test results (unpublished data from the program reported in reference 4), and the calculated optimal power-off descent from hover. An optimal flight path was not flown in the tests of course, and in addition some forward speed and cyclic flare were involved. Even so, the correlation is qualitatively good. The most important discrepancy is that the rotor speed in the flight tests does not initially decrease as fast as in the calculations. Examining the flight test data, it is found however that the engine torque does not decrease to zero immediately after the throttle chop; in fact, the torque remains above 25% of full power until the helicopter has descended about 15m. Adding to the analytical model an exponential lag in the engine power drop greatly improves the correlation in figures 4 and 5. While again one should not look for too much correlation here, the lower vertical load factor in the flight tests during the collective flare suggests that the ground effect might be stronger than was used in the model, perhaps due to the helicopter vertical velocity (the cyclic flare may be influencing the measured n_z also however).

CONCLUDING REMARKS

An optimal control solution has been obtained for the descent and landing of a helicopter after power loss. A comparison with flight test results shows sufficient correlation, even quantitatively, to verify the basic features of the model. The influences of parameters such as altitude and Lock number are correctly given, and the proper characteristics of the control technique are obtained. This model should thus prove to be a useful tool for evaluating and comparing the power-off landing characteristics of various helicopter designs.

REFERENCES

1. Gessow, Alfred and Myers, Garry C., Jr., Aerodynamics of the Helicopter, Frederick Ungar Publishing Co., New York, 1952

2. Cheeseman, I.C., and Bennett, W.E., "The Effect of the Ground on a Helicopter Rotor in Forward Flight," ARC R&M 3021, September 1955

3. Kirk, Donald E., Optimal Control Theory, Prentice-Hall, Inc., Englewood Cliffs, New Jersey, 1970

4. Wood, T.L., "High Energy Rotor System," 32nd Annual Forum of the American Helicopter Society, May 1976

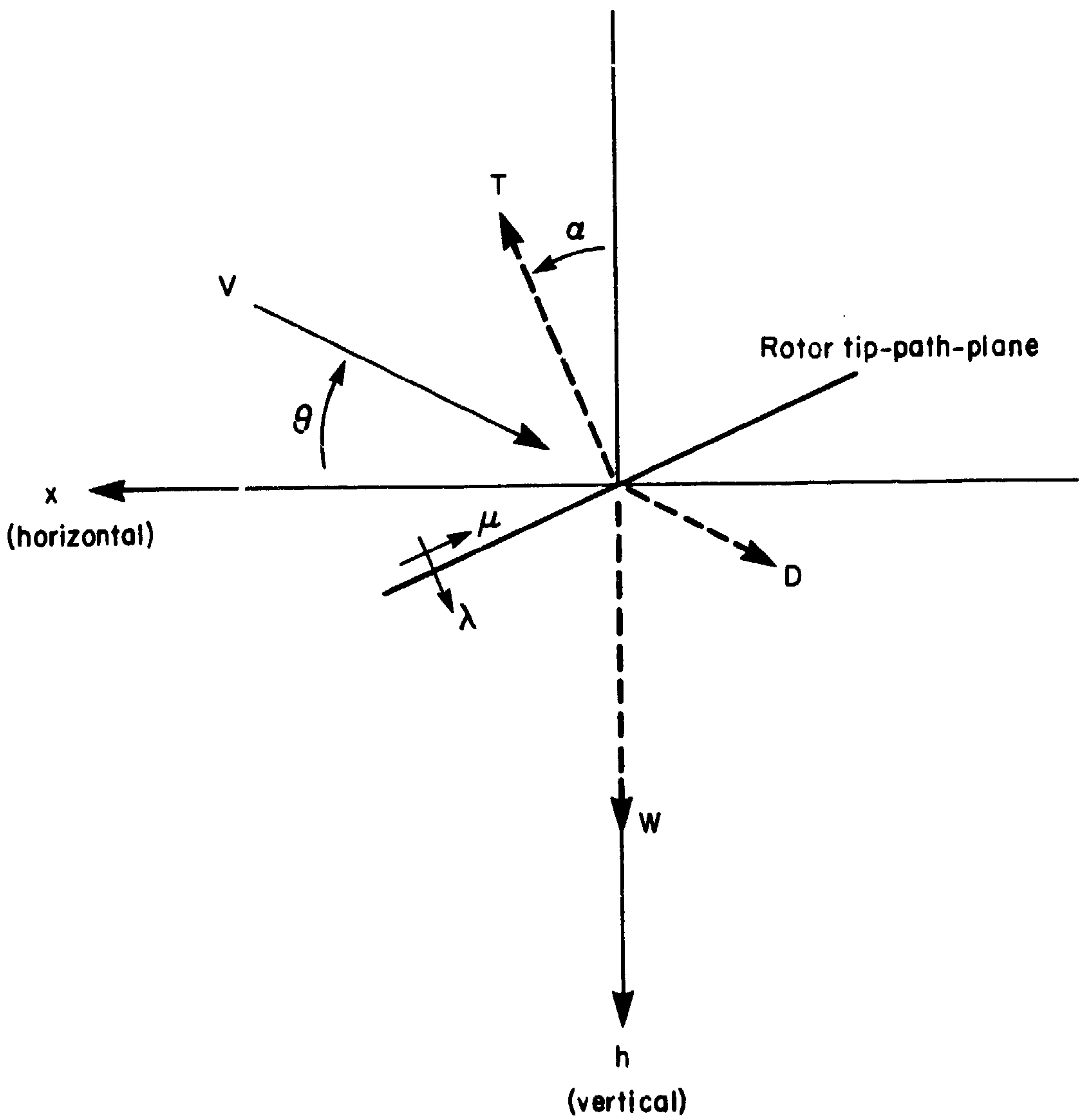

Figure 1 Definition of helicopter position (x and h), velocity (V and θ), and forces (W, D, T, and α).

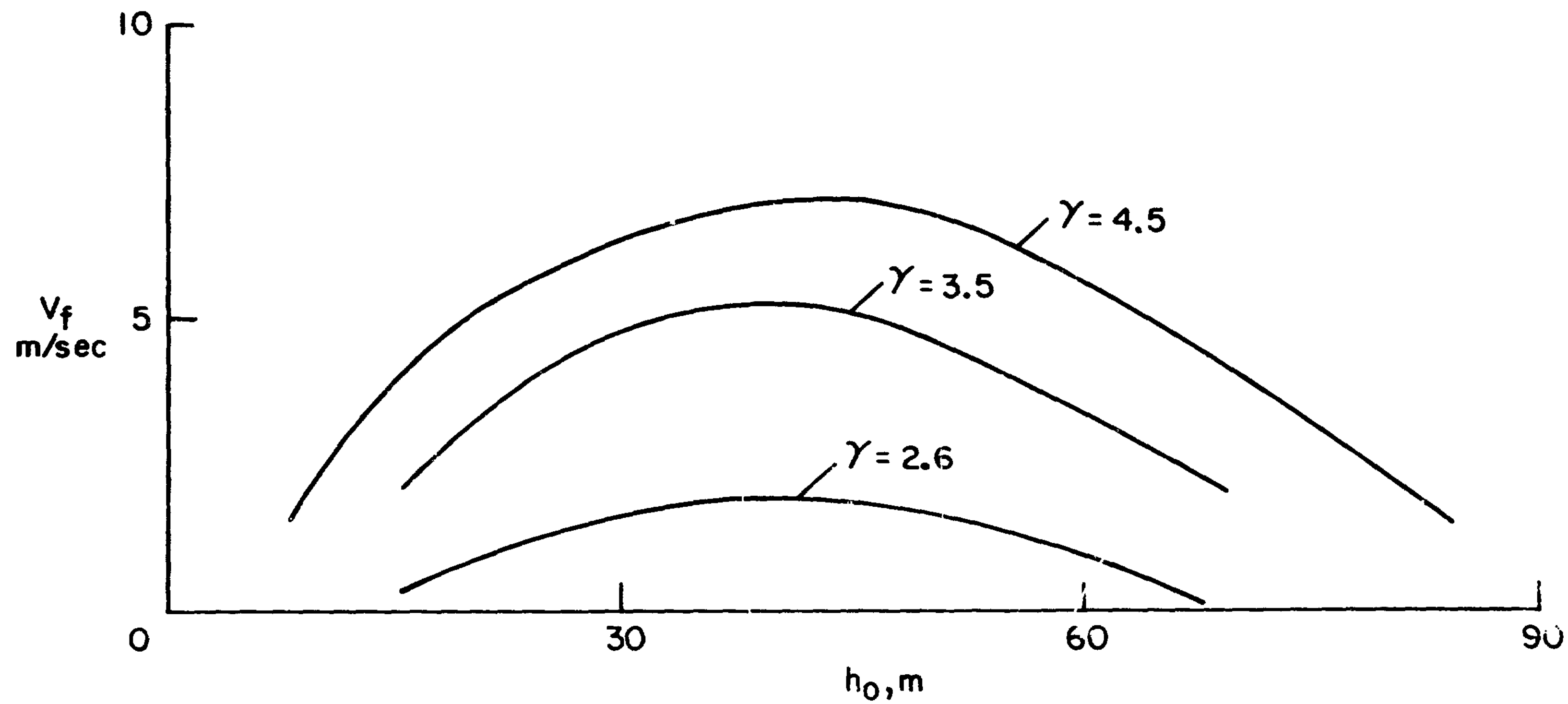

Figure 2 Vertical velocity at the ground after optimal power-off descent from hover at various altitudes, for three values of rotor Lock number γ ($R = 5.38$m, $\Omega R = 199$ m/sec, $C_T/\sigma_o = .063$, and $\sigma = .048$).

Figure 3 Optimal power-off descent from hover at altitude $h_o = 30$ m, for three values of rotor Lock number γ. ($R = 5.38$m, $\Omega R = 199$ m/sec, $C_T/\sigma_o = .063$, and $\sigma = .048$)

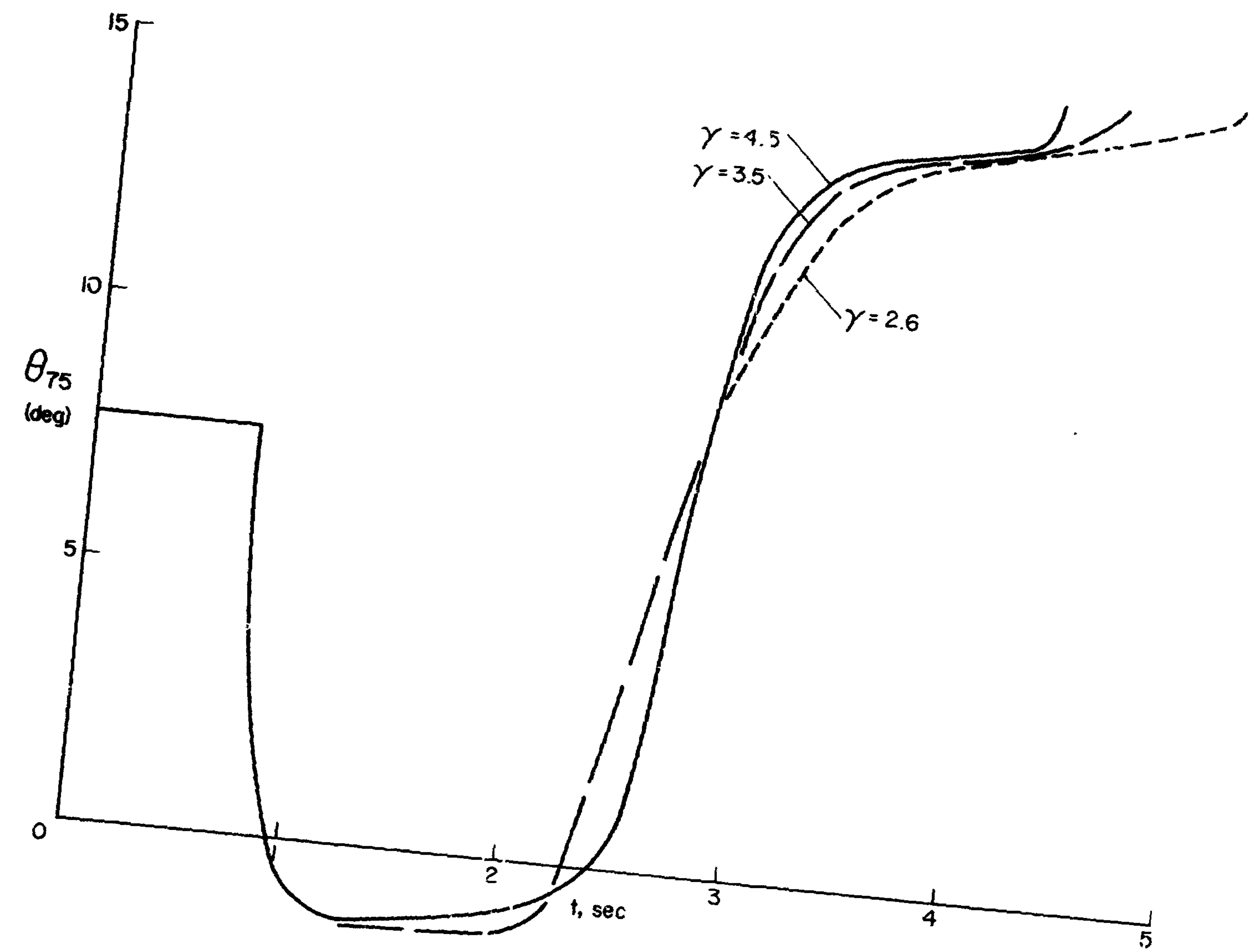

Figure 3(a). Collective pitch control.

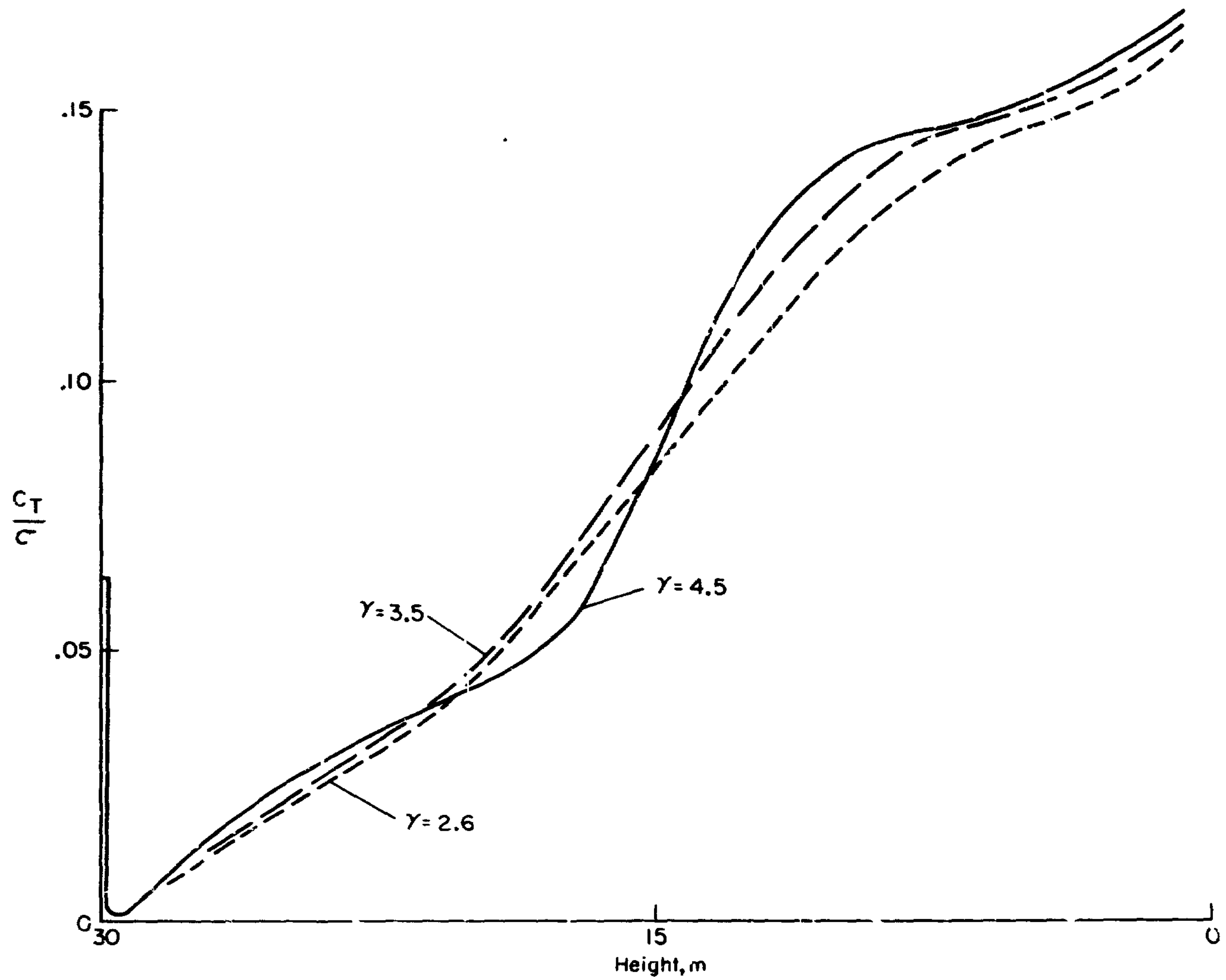

Figure 3(b). Rotor thrust coefficient to sclidity ratio.

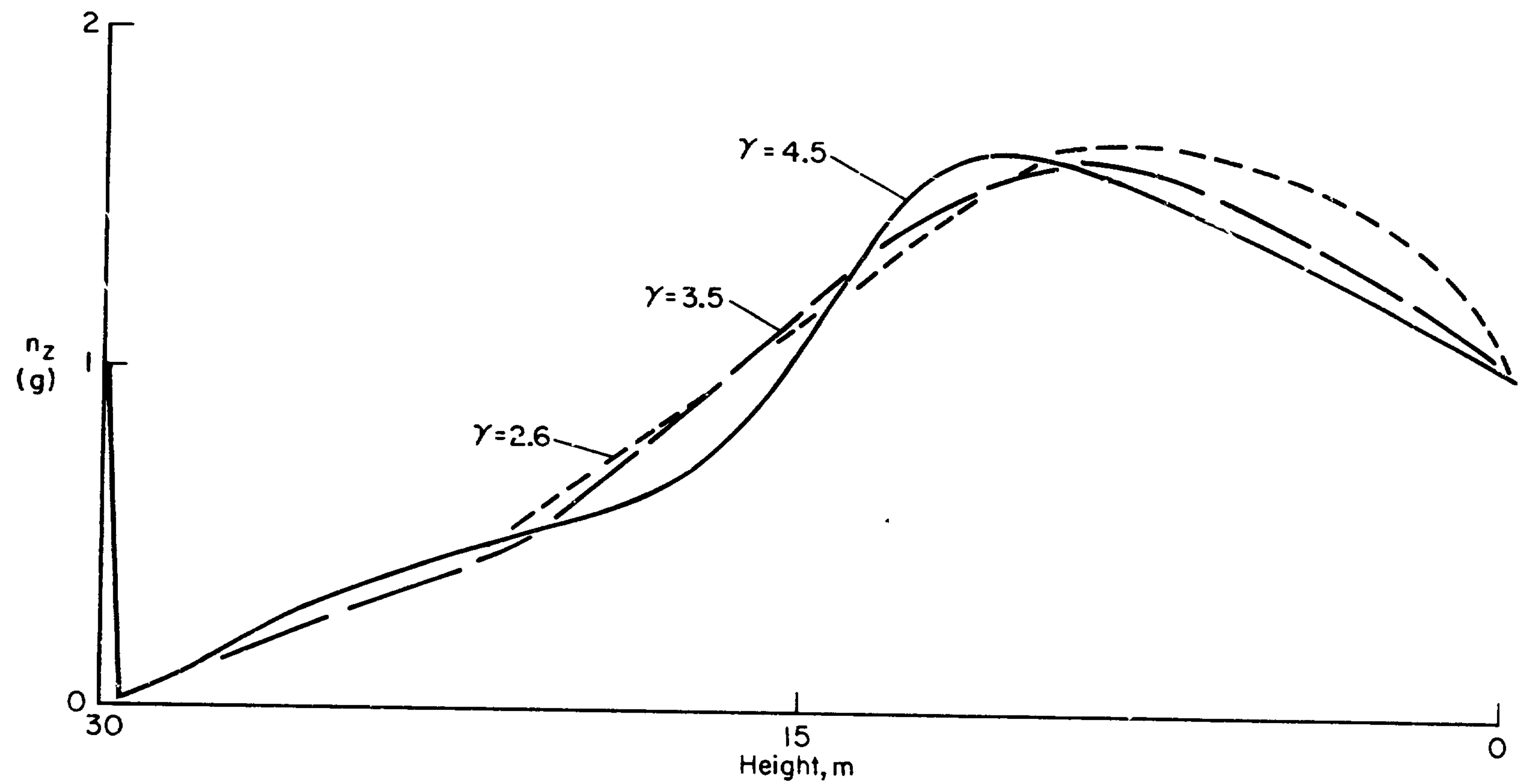

Figure 3(c). Helicopter vertical load factor.

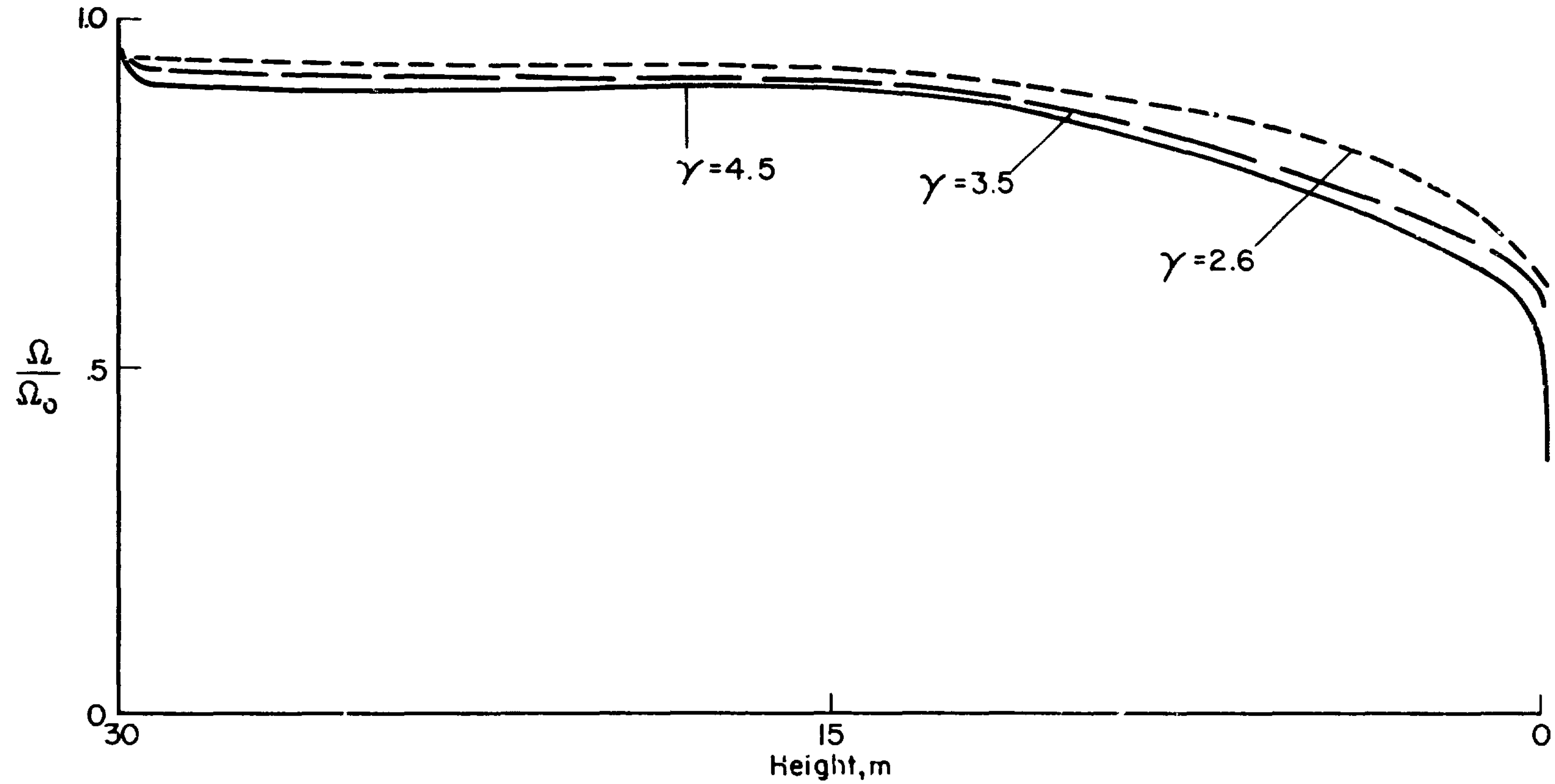

Figure 3(d). Rotor speed ratio.

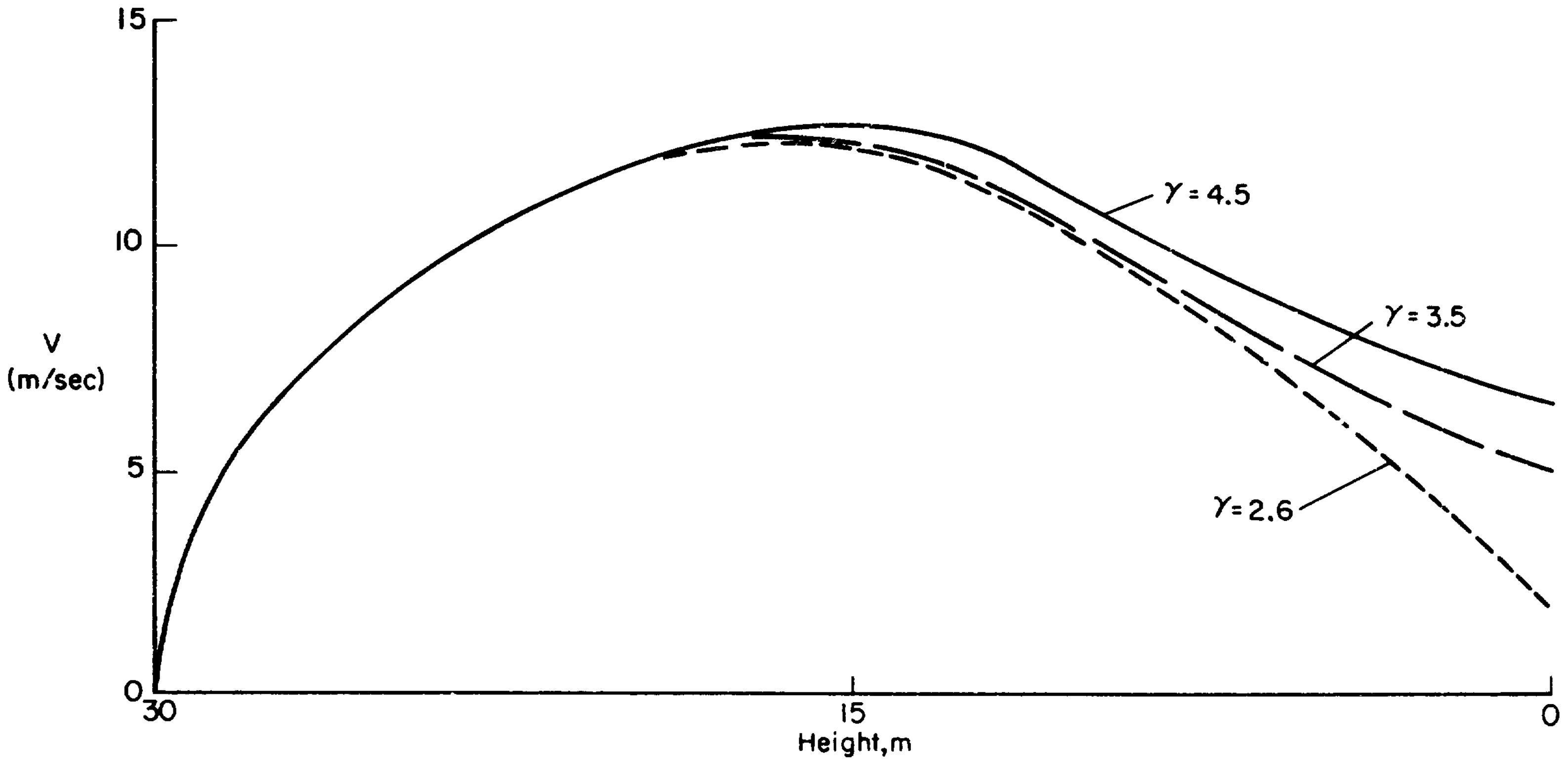

Figure 3(e). Vertical descent velocity.

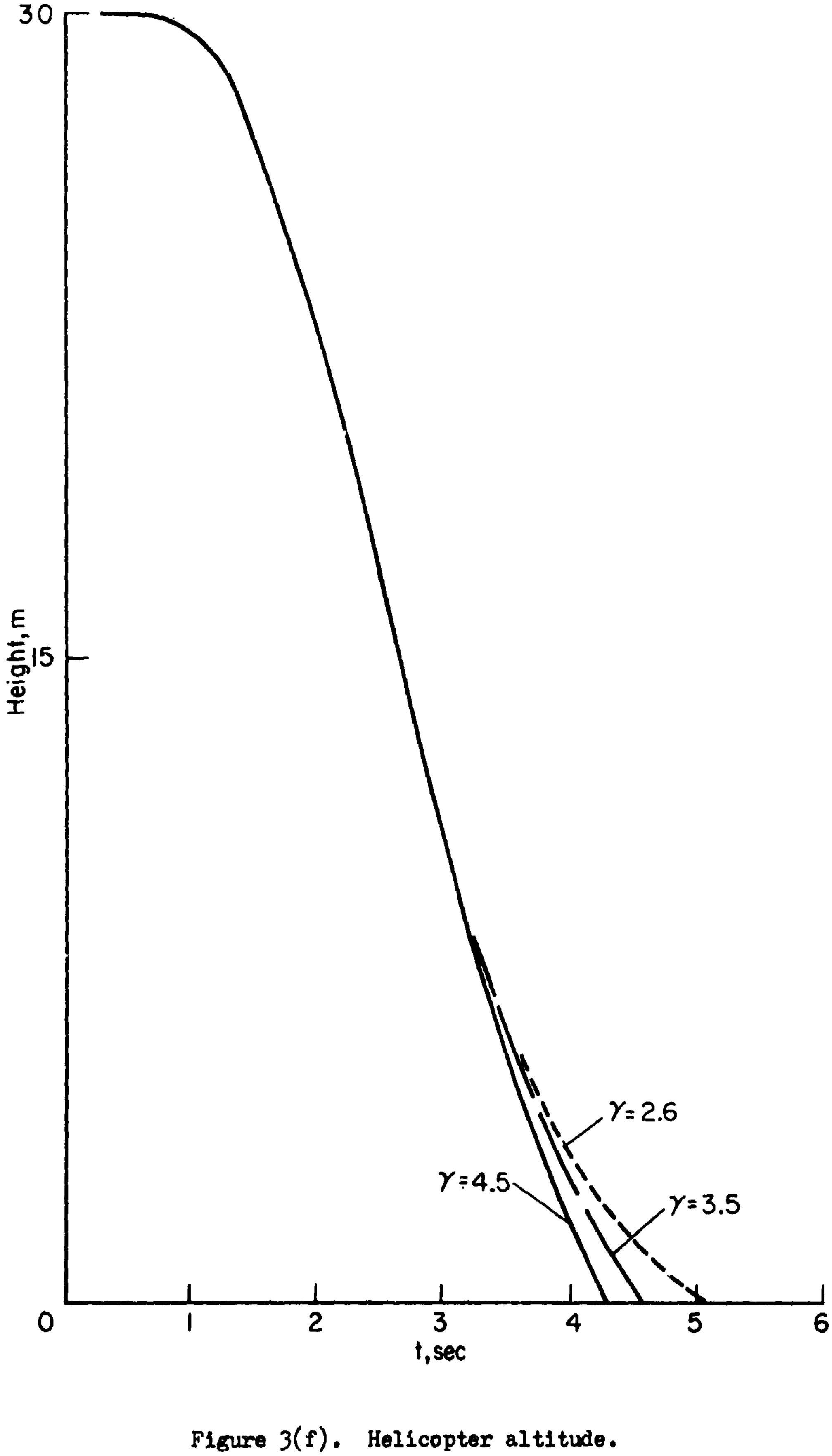

Figure 3(f). Helicopter altitude.

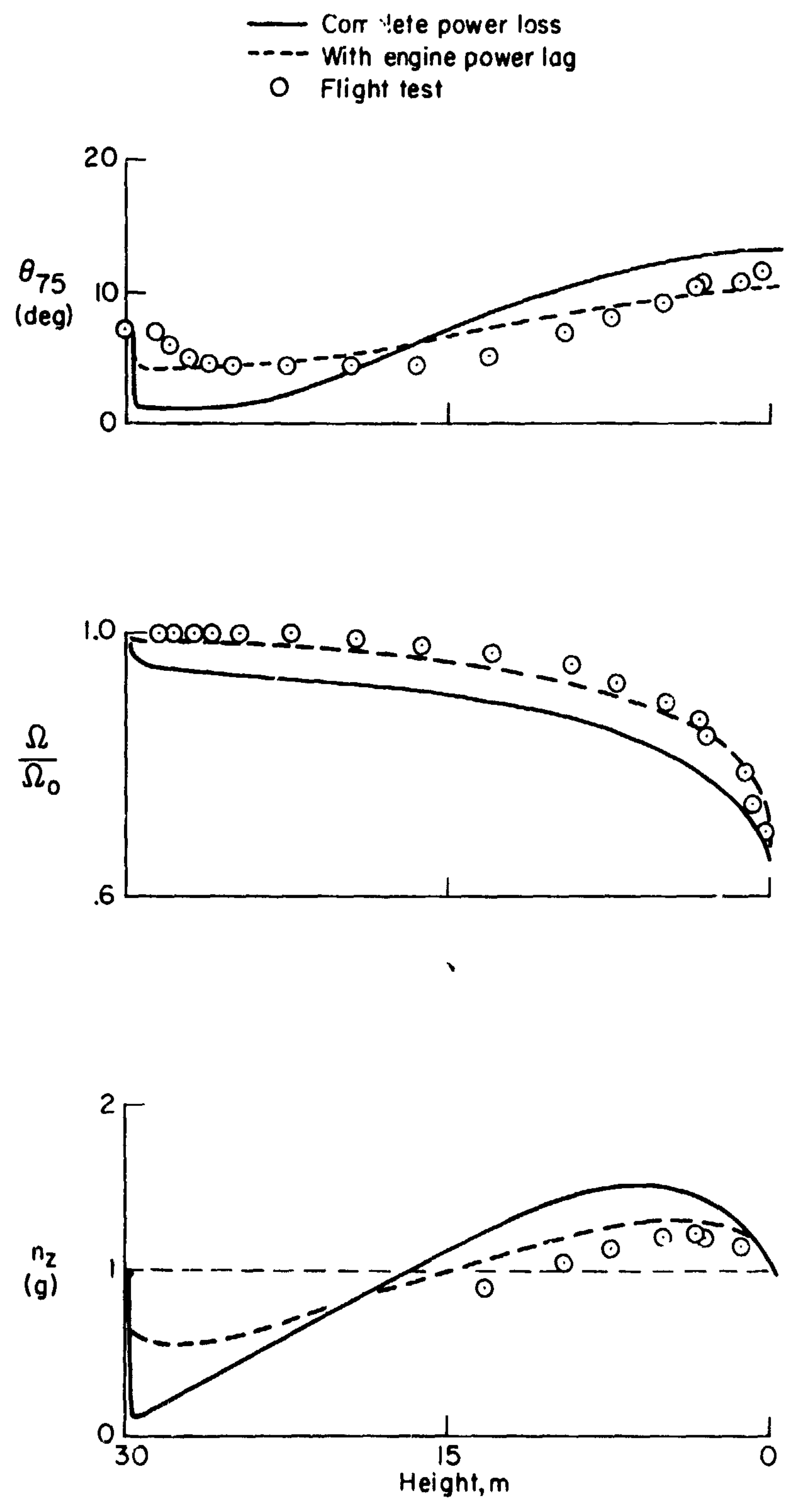

Figure 4 Comparison between flight test data and optimal power-off descent from hover at altitude $h_o = 30$ m. ($R = 5.38$ m, $\Omega R = 199$ m/sec, $C_T/\sigma_o = .057$, $\sigma = .048$, $\gamma = 2.6$)

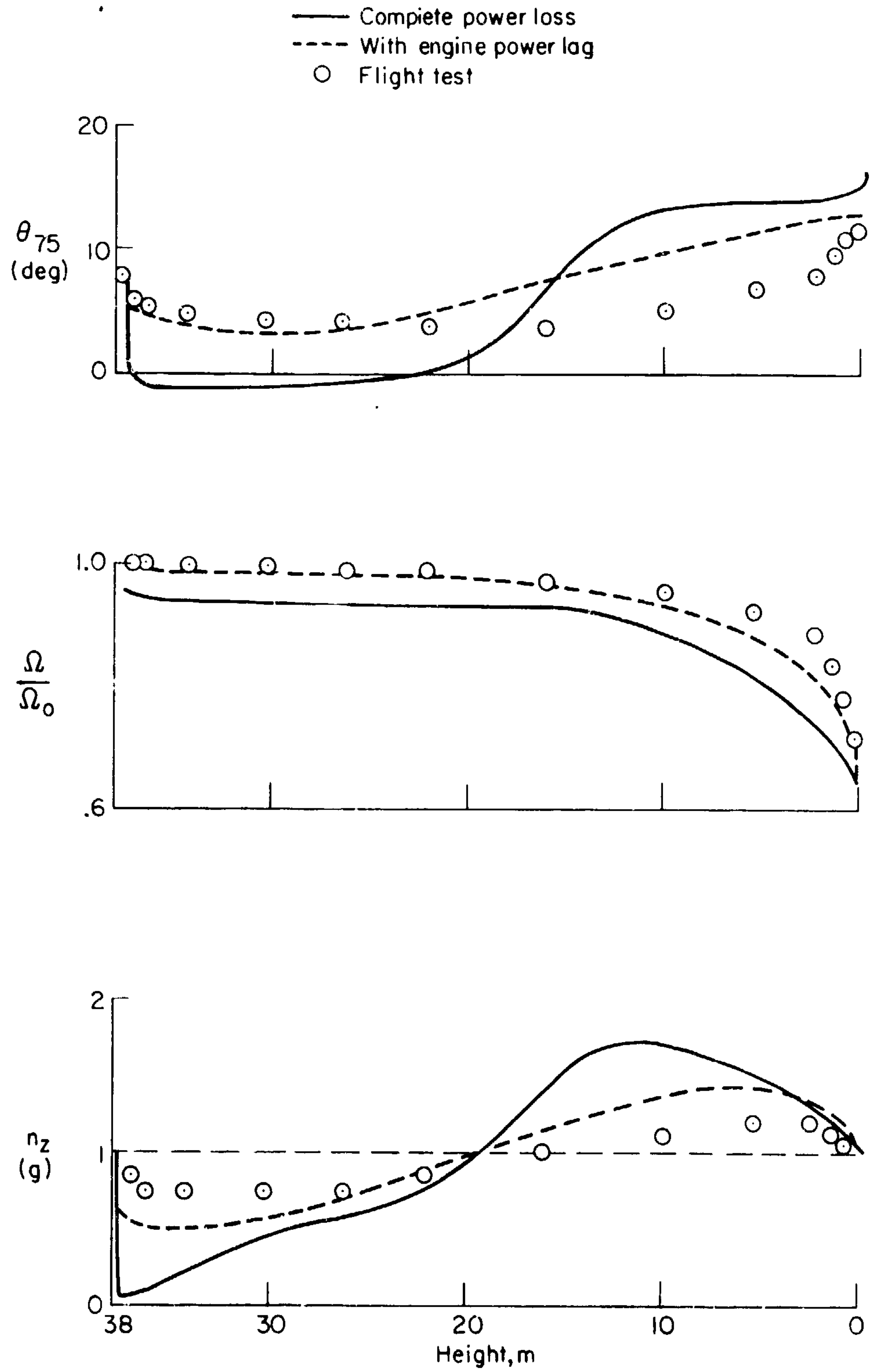

Figure 5 Comparison between flight test data and optimal power-off descent from hover at altitude h_o = 38 m. (R = 5.38m, ΩR = 199 m/sec, C_T/σ_o = .066, σ = .048, γ = 2.6)